Alma Mater Studiorum Università di Bologna
Archivio istituzionale della ricerca

Aqueous Au-Pd colloids catalyze selective CH4 oxidation to CH3OH with O2 under mild conditions

01 May 2024

Aqueous Au-Pd colloids catalyze selective CH$_4$ oxidation to CH$_3$OH with O$_2$ under mild conditions

Nishtha Agarwal[1], Simon J. Freakley[1], Rebecca U. McVicker[1], Sultan M. Althahban[2], Nikolaos Dimitratos[1], Qian He[1], David J. Morgan[1], Robert L. Jenkins[1], David J. Willock[1], Stuart H. Taylor[1], Christopher J. Kiely[1,2] and Graham J. Hutchings[1]*

[1] Cardiff Catalysis Institute, School of Chemistry, Cardiff University, Main Building, Park Place, Cardiff, CF10 3AT, UK.

[2] Department of Materials Science and Engineering, Lehigh University, 5 East Packer Avenue, Bethlehem, Pennsylvania, PA 18015, USA.

*Hutch@cardiff.ac.uk

Abstract

The selective oxidation of methane, the primary component of natural gas, remains an important challenge in catalysis. Using colloidal gold-palladium nanoparticles rather than the same nanoparticles supported on titanium oxide, we oxidized methane to methanol with high selectivity (92%) in aqueous solution at mild temperatures. Using isotopically labeled O_2 as an oxidant in the presence of H_2O_2, we demonstrate that the methanol produced incorporated a substantial fraction (70%) of gas-phase O_2. More oxygenated products were formed than H_2O_2 consumed, suggesting that the controlled breakdown of H_2O_2 activates methane which subsequently incorporates molecular oxygen through a radical process. If a source of methyl radicals can be established, then the selective oxidation of methane to methanol using molecular oxygen is possible.

In industry, CH₄ is used as a feedstock by first indirectly converting it to methanol (CH_3OH) via the production of synthesis gas ($CO + H_2$) at high temperatures and pressures, an expensive and energy intensive process *(1)*. The direct oxidation of CH_4 to CH_3OH, which is challenging as overoxidation must be avoided, has been the subject of intensive study for many decades *(2,3)*. Cyclic gas phase oxidation of CH_4 with metal-exchanged zeolite catalysts with O_2, N_2O or H_2O require high temperatures (200° to 500°C) to activate the oxidant and desorb product CH_3OH *(4-8)*. Liquid-phase reactions typically use milder reaction conditions; however, a closed catalytic cycle is often not achieved. Periana and co-workers reported that electrophilic metals such as Hg and Pt-complexes are active for methane oxidation *(9,10)*. These systems require high temperatures (180ºC) and strongly acidic media such as oleum to facilitate the reaction. Oxidation products are trapped as methyl-bisulphate to protect against overoxidation, which are then hydrolyzed to release methanol and SO_2. This catalyst was later heterogenized using a solid carbon framework to anchor the Pt catalyst *(11)*. Similarly, cationic Au in solution can oxidize CH_4 in the presence of even stronger oxidizing agents such as selenic acid which prevents the formation of metallic gold *(12)*.

More benign oxidants such as hydrogen peroxide (H_2O_2) with Fe-complexes have also been demonstrated to oxidize C-H bonds *(13)*. Yuan *et al.* previously showed activation of CH_4 with dissolved gold chloride and H_2O_2 at 90ºC, but observed agglomeration and precipitation of the catalyst from the solution *(14)*. Pd^{2+} was also reported to catalyse CH_4 oxidation to methyltrifluoroacetate using peroxytrifluoroacetic acid generated by H_2O_2 and trifluoroacetic anhydride *(15)*. Similarly, heterogeneous catalysts based on Fe-ZSM-5 and Cu modified ZSM-5 have been used for methane activation to methylhydroperoxide (CH_3OOH), CH_3OH, and formic acid (HCOOH) in aqueous media at 50 °C *(16)*. H_2O_2 is considered a desirable benign oxidant, second only to molecular O_2 for this reaction, as the side decomposition product is water.

We have also reported CH_4 oxidation using supported gold-palladium nanoparticles (NPs) under mild aqueous conditions using H_2O_2 as oxidant at 50 °C. The reaction proceeded through a radical mechanism as both methyl ($^\bullet CH_3$) and hydroxyl ($^\bullet OH$) radicals were observed by electron paramagnetic resonance (EPR) spectroscopy *(17)*. However, the relatively high cost of H_2O_2 for even stoichiometric oxidation of CH_4 makes it difficult to envisage a chemical process based on this chemistry that would be economically viable.

Incorporation of O_2 into the primary oxidation products would represent substantial progress toward a feasible CH_4 to CH_3OH process. Here we report this reaction under mild conditions using colloidal AuPd NPs in the presence of both H_2O_2 and O_2. We show that by removing the support material from the catalyst, a substantial improvement in activity is achieved and O_2 is incorporated into the primary products, with the selectivity to primary products reaching >90% with minimal CO_2 produced.

We prepared polyvinylpyrrolidone (PVP) stabilized AuPd (1:1 molar ratio) colloids and supported catalysts by immobilizing the colloid on TiO_2 (see Supplementary Material for all experimental details) (*18, 19*). We investigated CH_4 oxidation was investigated in water with H_2O_2 as oxidant at 50 °C and 30 bar CH_4 for 30 min *(19)*. With the supported colloid material, 1% AuPd/TiO_2 catalyst (Table 1, Entry 1), minimal reaction products were observed (primary oxygenate selectivity 26%) as determined by quantitative nuclear magnetic resonance (NMR) analysis (*16,19*). In this experiment, most of the H_2O_2 was decomposed (73%). A gain factor, defined as the mol oxygenate produced /mol H_2O_2 consumed, was calculated to be 2×10^{-3}.

This high rate of H_2O_2 degradation was considered detrimental to the reaction either by (i) the termination of reactive radical chains caused by radical concentrations being too high or (ii) by consumption of H_2O_2 at such a high rate that it does not allow sufficient interaction with the low amount of solubilized CH_4. We investigated which component of the catalyst was responsible for the high H_2O_2 degradation rates. We observed (Fig. S1) that the degradation of H_2O_2 at room temperature under atmospheric pressure was low in the presence of bare TiO_2 and unsupported AuPd colloidal NPs. Only when the AuPd NPs were supported on TiO_2 did the catalyst exhibit a high rate of H_2O_2 degradation, suggesting that either the interfacial sites at the support/metal interface (*20*) or a change in the morphology of the NP (*21*) upon immobilization led to the high H_2O_2 degradation rates (*22*).

This finding, coupled with the known ability of high surface area TiO_2 to quench radical reactions (*23*), led us to evaluate the ability of unsupported PVP-stabilized AuPd colloids to catalyze CH_4 oxidation. We utilized 1000 μmol H_2O_2, and using the same amount of metal as in the supported catalyst, observed substantially more product (15.7 μmol) compared to the supported catalysts (Table 1, entry 2), while much less H_2O_2 (38%) was consumed. Furthermore, the primary products, CH_3OOH and CH_3OH, were produced with 90% selectivity. The colloidal catalyst was an order of magnitude more efficient than the solid

AuPd/TiO$_2$ catalyst with respect to products generated per unit amount of H$_2$O$_2$ consumed, with a gain factor of 3×10^{-2} compared to 2×10^{-3}.

The presence of CH$_3$OOH, CH$_3$OH, HCOOH and CO$_2$ in the product stream suggests a consecutive oxidation pathway, as previously observed *(16, 17)*. Experiments with isotopically labeled ^{13}CH$_4$ confirmed that the carbon source was CH$_4$ and not the organic stabilizer, PVP, present in the colloidal solution (Fig. S2). Carbon-based products containing the label were present in quantities corresponding to the amount of labeled ^{13}CH$_4$ present; in addition, no carbon-based products were observed when CH$_4$ was not present (Table S1).

STEM-HAADF (Scanning transmission electron microscopy- high angle annular dark field) imaging of the fresh AuPd-PVP colloids showed them primarily to have multiply-twinned icosahedral structures, although some cuboctahedral NPs were also detected (Fig. 1, A and B). The AuPd-PVP colloids ranged in size between ~2 and 12 nm and had a mean diameter of 3.7 nm (Fig. 1C). STEM-XEDS (X-ray energy dispersive spectroscopy) compositional analysis showed the AuPd-PVP NPs to have a similar Au:Pd ratio irrespective of their size (Fig. S3). Transmission electron microscopy (TEM) analysis of the sol-immobilized AuPd/TiO$_2$ samples (Fig. S4) showed the AuPd NPs to have a similar size, morphology, and composition to their colloidal counterparts. X-ray photoelectron spectroscopy (XPS) analysis of both the supported and colloidal samples showed that both Au and Pd were metallic in nature with minor PdCl$_2$ components detected in the colloidal samples (Figs. S5 & S6).

Previous EPR spin-trapping studies revealed the presence of both $^{\bullet}$OH and $^{\bullet}$CH$_3$ radicals during reactions with a sol-immobilized AuPd catalyst suggesting that the reaction mechanism is radical based *(17,24)*. The observation that the primary product was CH$_3$OOH implies that the primary termination step is either between $^{\bullet}$CH$_3$ and $^{\bullet}$OOH radicals or from recombination of $^{\bullet}$CH$_3$ with dissolved O$_2$ in the solution originating from the decomposition of H$_2$O$_2$ *(25)*. In the case of the unsupported colloidal catalyst, which decomposes H$_2$O$_2$ at a much slower rate but makes substantially more products, we rationalized that $^{\bullet}$CH$_3$ was being produced over a longer time-scale and that adding O$_2$ to the reaction mixture would promote oxygen incorporation through the generation of $^{\bullet}$CH$_3$OO radicals. The reaction of $^{\bullet}$CH$_3$ with O$_2$ has been reported to occur at high rates in gas-phase reactions *(26)*. The addition of 5 bar of O$_2$ (Table 1, Entry 3) to the reaction resulted in an increased product yield (26.8 μmol) compared to the H$_2$O$_2$ only reaction (Table 1, Entry 2) while maintaining a high selectivity to primary oxygenates (95%). The gain factor also remained an order of magnitude higher

5

than that of the supported catalyst and was more than doubled that of the colloidal catalyst with H_2O_2-only. These results suggest that the presence of additional of O_2 (beyond that originating from H_2O_2 decomposition) promoted the termination steps that generate primary products.

To demonstrate the incorporation of O_2 into the primary products using the colloidal catalyst at 5 bar, $^{18}O_2$ was added to the reaction mixture. Solutions from isotopic labeling reactions were analyzed by gas chromatography-mass spectrometry (GC-MS) which resulted in the degradation of the CH_3OOH primary oxidation product to CH_3OH due to the high injection temperature; however, good agreement was observed between the combined amount of CH_3OOH and CH_3OH determined by NMR and the amount of CH_3OH determined by GC-MS (Fig. S7). Mass spectrometry analysis of the reactions using $H_2^{16}O_2$ and $^{18}O_2$, revealed that CH_3OH mass fragments containing the ^{18}O label were responsible for 51% of the observed signal. (Fig. S8). Reactions in the absence of H_2O_2 at 50 °C (Table 1, Entry 4) showed no generation of oxygenated products confirming that H_2O_2 was a necessary ingredient for the reaction to take place. These results show that under mild aqueous reaction conditions, colloidal AuPd NPs can catalyze the reaction of H_2O_2 + CH_4 + O_2 with incorporation of O_2 into the primary reaction products.

We investigated decreasing the amount of H_2O_2 used in order to increase efficiency with the aim of generating more than one primary oxygenate species per molecule of H_2O_2 consumed. Figure 2A shows that by decreasing the amount of H_2O_2 from 2000 to 1000 μmol over 60 mins while maintaining 5 bar O_2 in the gas phase, the quantity of products formed initially increased from 18 to 43 μmol. This increase coincided with a reduction in the amount of H_2O_2 consumed (from 81% to 64%) indicating that a much greater efficiency was achieved with less H_2O_2, (a full breakdown of products is given in Table S2).

For a radical mechanism, an excess of H_2O_2 could likely cause termination of radical reactions and limiting product formation. A further reduction in the amount of H_2O_2 from 1000 to 500 μmol resulted in a slight increase in reaction products from 43 to 50 μmol suggesting the reaction had become limited by the availability of a reactant other than the radical species generated by H_2O_2, *i.e.,* either O_2 or CH_4 as determined by their solubility in the aqueous reaction media. Decreasing the amount of H_2O_2 further resulted in lower consumption of H_2O_2, but also led to a decrease in product formation, probably because of a reduction in the concentration of radicals generated. For the optimized amount of H_2O_2 (50

6

µmol) (Table 1, entry 5) the gain factor, reached 1.2, and represents an increase by three orders of magnitude over the corresponding 1% AuPd/TiO$_2$ sol-immobilized catalyst together with a higher selectivity to primary oxygenates. Furthermore, $^{18}O_2$ isotopic labeling experiments carried out under these optimized conditions again revealed substantial incorporation of $^{18}O_2$ (*ca.* 50%) into the primary products (Fig. S9).

In all the isotopically labelled reactions, CH$_3$OOH was decomposed to CH$_3$OH during the analysis. To ensure that thermal decomposition did not result in loss of the isotopic label, we quantitatively (confirmed by NMR analysis) reduced CH$_3$OOH to CH$_3$OH with NaBH$_4$ before performing GC-MS analysis. Using this procedure to prevent thermal decomposition of CH$_3$OOH in the presence of atmospheric oxygen, more than 70% of the CH$_3$OH detected showed incorporation of the ^{18}O label (Fig. 2B). In the previous isotope labeling experiments, radical decomposition of labelled CH$_3$OOH in the presence of air and any remaining H$_2$O$_2$ resulted in an underestimate of the degree of ^{18}O incorporation (*27*).

We conducted control experiments with unsupported monometallic Au and Pd colloids, along with the corresponding precursor metal chlorides using the same metal concentration of 6.6 µmol under identical reaction conditions (Table 1, entries 6-9). The monometallic Au and Pd colloids as well as the metal chloride precursors showed no activity for CH$_4$ oxidation. In fact, the HAuCl$_4$ and Pd colloid precipitated during the reaction. Hence, alloyed AuPd NPs show a synergistic effect in terms of activity and stability for this reaction. Recently, leaching of precious metals into reaction solutions to generate clusters containing 3 to 5 atoms has been implicated in catalytic reactions and characteristically show an induction period at the start of the reaction as the clusters form (*28*). HAADF-STEM analysis of the used colloid, showed some limited particle growth, but no evidence of subnanometer clusters or isolated Au-atoms was found either before or after 30 min of reaction under optimized reaction conditions (Fig. 1, D to F).

Furthermore, no substantial differences in the concentrations of cationic Au or Pd content were observed by XPS measurements on pre- or post-reaction AuPd-PVP colloids (Fig. S5). Time-on-line analysis indicates that there is no induction period associated with this reaction system and that products were generated even before the 50°C reaction temperature was reached. The catalyst being colloidal rather than a solid powder likely removed some mass transfer limits that create an induction period (Fig. 2C). This observation, coupled with inactivity of the monometallic Au- and Pd- sols and metal chloride precursors, indicates that

7

the bimetallic colloidal NPs are the active catalyst. The presence of reaction products at the start of the reaction (*i.e.,* just after completion of the heating ramp at 2.25°C/min) suggests that there is some activity at even lower temperatures. As the reaction proceeded, the total amount of product generated plateaus at ~120 min (Fig. 2C, Table S3) which coincided with the depletion of H_2O_2 from the reaction mixture. After adding more H_2O_2, more products were generated and a similar oxidation rate was achieved, indicating that the AuPd colloid was stable during this time (Fig. 2C, Table S4).

As the reaction time was increased further, some overoxidation of the primary products was observed, but the level of CO_2 production remained at < 4% of the total products formed over the entire 240 min duration (Table S4, Entry 4). We also conducted reactions at room temperature both with and without the addition of 5 bar O_2 as part of the reaction mixture and observed activity with similar levels of primary oxygenate selectivity (96%). A gain factor 1.35 is observed at room temperature in presence of O_2 (Fig. 2d) similar to the reaction performed at 50°C in the presence of O_2 (Table S5) producing 5.4 µmol of products with only 4 µmol H_2O_2 consumption, corresponding to a productivity of 10.4 $mol_{oxygenates}$ kg_{cat}^{-1} h^{-1}. This productivity compares favorably with that reported for methane monooxygenase (pMMO) from *M. capsulatus* (Bath) (5.05 $mol_{methanol}$ kg^{-1} h^{-1}) (*29*), a biological system that selective oxidizes CH_4.

Preliminary kinetic analysis shows a first order dependence on colloid, CH_4 and H_2O_2 concentration (Figure S10) indicating a rate determining step including CH_4 and H_2O_2 with an observed activation energy of 39 kJ mol^{-1}. Because the reaction only proceeds when H_2O_2 is present in the reaction mixture, the initial activation of CH_4, to $^{\bullet}CH_3$ is likely to occur through a radical mechanism (Scheme 1), a process that is suppressed by the presence of a catalyst support such as TiO_2 (see Table S6 for this comparison). These $^{\bullet}CH_3$ radicals can react quickly with dissolved O_2, which results in incorporation of >70 % O_2 into the primary reaction products under optimized conditions. Some products containing ^{16}O were formed through radical reactions between $^{\bullet}CH_3$ with either $^{\bullet 16}O^{16}OH$ or $^{16}O_2$ generated from the decomposition of $H_2^{16}O_2$. The $^{\bullet}CH_3$ radicals were generated via hydrogen abstraction by $^{\bullet}OH$ from H_2O_2 and this initiation step activates CH_4 (Scheme 1). In the optimized reaction, 10 µmol H_2O_2 and 5 bar $^{18}O_2$ were required to generate 20 µmol, where the primary products contained 70% ^{18}O (14 µmol) and 30% ^{16}O (6 µmol). These isotopic ratios and the reaction scheme proposed are broadly in-line with the total amount of H_2O_2 consumed (16 µmol), where 10 µmol was used to generate $^{\bullet}CH_3$ radicals and 6 µmol was used in ^{16}O products via

decomposition. Greater efficiency was achieved in terms of O_2 incorporation, by utilizing H_2O_2 to activate CH_4 rather than using it to supply oxygen into the primary products. Although CH_4 activation via $^\bullet OH$ was required for formation of $^\bullet CH_3$ radicals, once formed, they readily reacted with O_2 to form CH_3OH

With this mechanism in mind, we tested an iron-based Fenton's type catalyst with H_2O_2 to investigate if $^\bullet OH$ in the absence of the AuPd colloid could activate methane, but negligible product formation was observed (Table S7). Therefore, the presence of the AuPd colloidal nanoparticles are also essential for CH_4 activation. We propose that in principle, other routes for the generation of $^\bullet CH_3$ radicals could be used to facilitate this chemistry. For example, rather than using H_2O_2, it would be highly desirable to devise a method of coupling the AuPd colloidal catalyst with a photochemical *(30, 31)* or electrochemical fuel cell *(32, 33)* to generate $^\bullet OH$ for H abstraction in order to facilitate $^\bullet CH_3$ radical formation.

Table 1. Catalytic activity. Comparison of catalytic activity of supported and unsupported colloidal Au-only, Pd-only and AuPd catalysts for the liquid phase oxidation of CH_4 using H_2O_2. *Test conditions:* Reaction time = 0.5 h; Stirring speed = 1500 rpm; Pressure CH_4= 30 bar; Reaction temperature =50 °C with stirred heating ramp rate of 2.25 °C/min.

Entry	Catalyst	H_2O_2 µmol	O_2 bar	Amount of Product (µmol)				Primary Oxygenate Selectivity / %	Oxygenate Productivity /mol kg_{cat}^{-1} h^{-1}	H_2O_2 Consumed / %	Gain Factor
				CH_3OOH	CH_3OH	HCOOH	CO_2				
1	1%AuPd/TiO_2	1000	0	0.0	0.4	0.00	1.2	26	0.03	73	2×10^{-3}
2	AuPd colloid	1000	0	11.8	3.3	0.6	1.1	90	29.4	38	3×10^{-2}
3	AuPd colloid	1000	5	17.4	7.6	1.8	1.5	88	53.6	27	9×10^{-2}
4	AuPd colloid	0	5	0	0	0	0.2	0	0	0	-
5	AuPd colloid	50	5	15.7	2.8	1.2	0.3	92	39.4	44	1.2
6	Pd colloid	50	5	0	0	0	0.7	0	0	22	0
7	Au colloid	50	5	0	0	0	0.1	0	0	12	0
8	$PdCl_2$	50	5	0	0	0	0.3	0	0	5	0
9	$HAuCl_4$	50	5	0	0	0	0.2	0	0	10	0

Entry 1: Sol-immobilized solid catalyst, 100 mg (6.6 µmol metal in 10 mL water)
Entries 2-7: Colloidal catalysts (10 mL, 6.6 µmol of metal)
Entries 8, 9: Homogeneous metal precursor solutions (6.6 µmol metal in 10 mL water)

Figure 1. Catalyst characterization. Representative HAADF images and particle size distributions for the unsupported AuPd-PVP sol in the fresh (**A to C**) and after a CH$_4$ oxidation reaction (**D to F**).
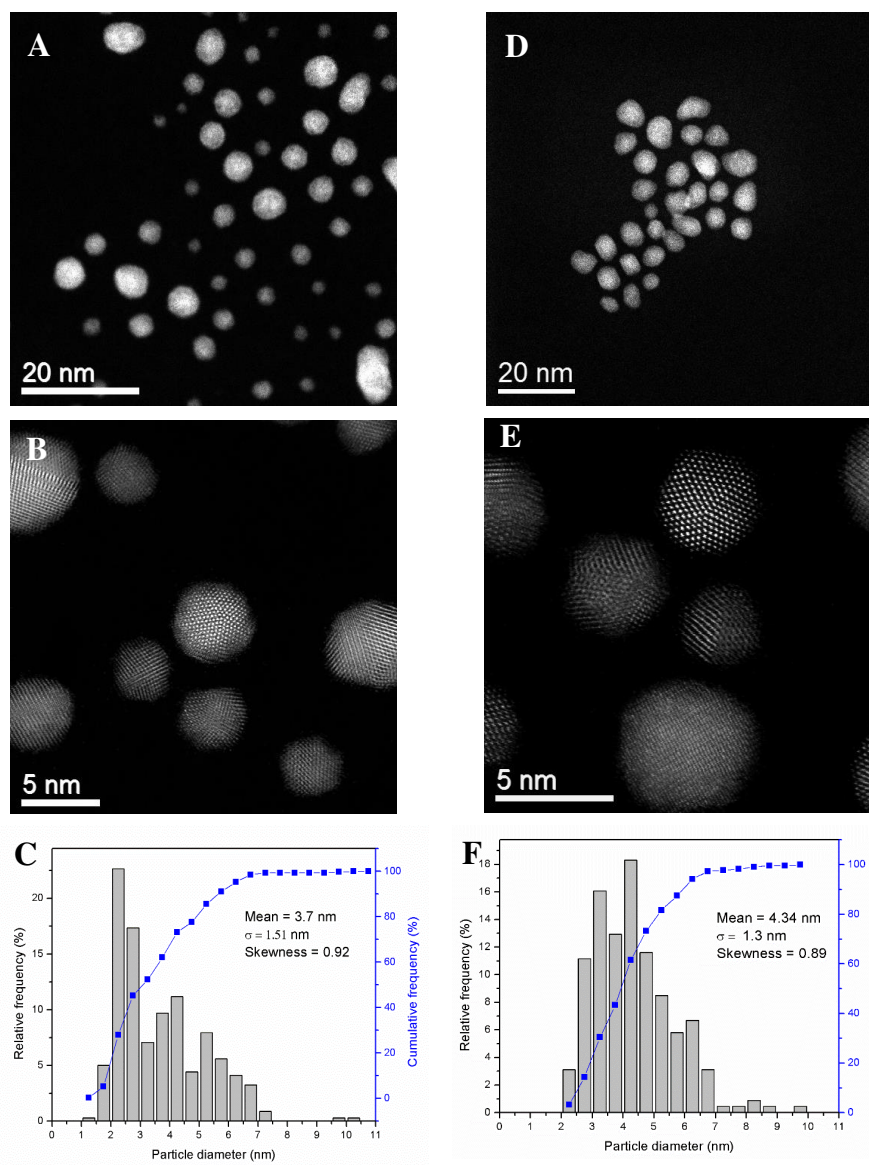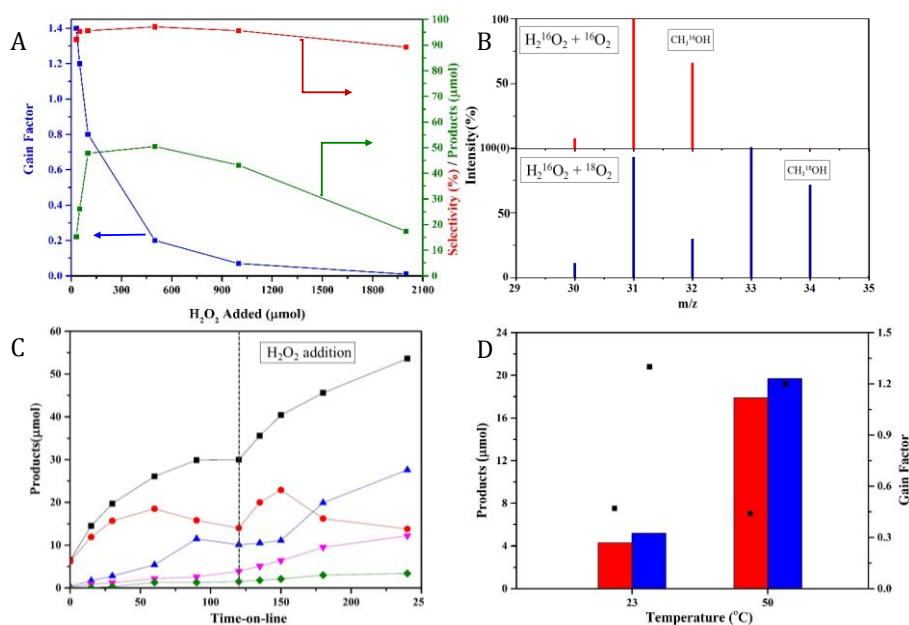
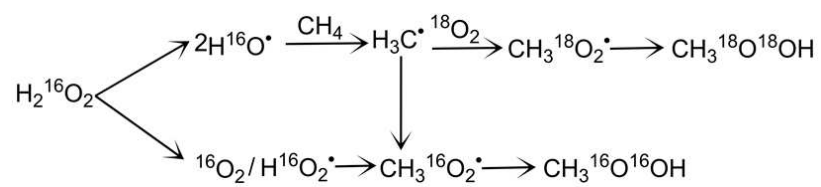**Figure 2. Methane oxidation reactions carried out over unsupported AuPd colloids.**

(A) Gain factor (blue line), selectivity (red line) and total amount of products (green line) as a function of the different amounts of H_2O_2 used.

(B) GC-MS spectra of CH_3OH formed (m = 32 and 34 for $CH_3^{16}OH$ and $CH_3^{18}OH$ respectively) during methane oxidation with a AuPd colloid via $H_2^{16}O_2 + {}^{16}O_2$ (*upper spectrum)* or $H_2^{16}O_2 + {}^{18}O_2$ (*lower spectrum*). For CH_4 oxidation with ${}^{18}O_2$, > 70% of ${}^{18}O_2$ molecules were incorporated in the CH_3OH product.

(C) Time-on-line and AuPd colloid re-use study for the methane oxidation reaction employing 50 µmol H_2O_2 and 5 bar O_2 showing no induction period. Total products (black line), and individual products (CH_3OOH (red line), CH_3OH (blue line), $HCOOH$ (pink line) and CO_2 (green line)) generated as a function of time-on-line. The black dotted vertical line at 120 min indicates a subsequent second addition of H_2O_2.

(D) Oxidation of CH_4 performed at 23° and 50°C with 50 µmol H_2O_2. The blue and red bars represent reactions performed with and without 5 bar O_2, respectively. The black squares (■) indicate their respective gain factors.

Scheme 1. Proposed reaction scheme for methane oxidation in the presence of H$_2$O$_2$ and molecular O$_2$.

$H_2{}^{16}O_2$

$\nearrow 2H^{16}O^{\bullet} \xrightarrow{CH_4} H_3C^{\bullet} \xrightarrow{{}^{18}O_2} CH_3{}^{18}O_2{}^{\bullet} \longrightarrow CH_3{}^{18}O^{18}OH$

$\searrow {}^{16}O_2 / H^{16}O_2{}^{\bullet} \longrightarrow CH_3{}^{16}O_2{}^{\bullet} \longrightarrow CH_3{}^{16}O^{16}OH$

References

1. International Energy Agency, (IEA), "Resources to Reserves" (IEA Publication ISBN 978-92-64-08354-7, 2013; www.iea.org/publications/freepublications/publication/Resources2013.pdf).

2. H. D. Gesser, N. R. Hunter, C. B. Prakash, The direct conversion of methane to methanol by controlled oxidation. *Chem Rev*. **85**, 235-244 (1985).

3. B. L. Conley *et al*. Design and study of homogenous catalysts for the selective, low temperature oxidation of hydrocarbons. *J. Mol. Cat. A: Chem.* **251**, 8-23 (2006).

4. V. I. Sobolev, K. A. Dubkov, O. V. Panna, G. I. Panov, Selective oxidation of methane to methanol on a Fe-ZSM-5 surface. *Catal. Today* **24**, 251-252 (1995).

5. E. V. Starokon *et al.*, Oxidation of methane to methanol on the surface of Fe-ZSM-5 zeolite. *J. Catal.* **300**, 47–54 (2013).

6. M. H. Groothaert, P. J. Smeets, B. F. Sels, P. A. Jacobs, R. A. Schoonheydt, Selective oxidation of methane by the bis(μ-oxo)dicopper core stabilized on ZSM-5 and mordenite zeolites. *J. Am. Chem. Soc.* **127**, 1394-1395 (2005).

7. T. Sheppard, C. D. Hamill, A. Goguet, D. W. Rooney, J. M. Thompson, A low temperature, isothermal gas-phase system for conversion of methane to methanol over Cu-ZSM-5. *Chem. Comm.* **50**, 11053-11055 (2014).

8. V. L. Sushkevich, D. Palagin, M. Ranocchiari, J. A. Van Bokhoven, Selective anaerobic oxidation of methane enables direct synthesis of methanol. *Science* **356,** 523-527 (2017).

9. R. A. Periana *et al.*, A mercury-catalyzed, high-yield system for the oxidation of methane to methanol. *Science* **259**, 340-343 (1993).

10. R. A. Periana *et al.*, Platinum catalysts for the high-yield oxidation of methane to a methanol derivative. *Science* **280**, 560-564 (1998).

11. R. Palkovits, M. Antonietti, P. Kuhn, A. Thomas, F. Schüth, Solid catalysts for the selective low-temperature oxidation of methane to methanol. *Angew. Chem. Int. Ed..* **48**, 6909-6912 (2009).

12. C. J. Jones *et al.*, Selective oxidation of methane to methanol catalyzed, with C-H activation, by homogeneous, cationic gold. *Angew. Chem. Intl. Ed.* **116**, 4726-4729 (2004).

13. G. B. Shul'pin, G. V. Nizova, Y. N. Kozlov, C. L. Gonzalez, G. Süss-Fink, Hydrogen peroxide oxygenation of alkanes including methane and ethane catalysed by iron complexes in acetonitrile. *Adv. Synth. Catal.* **346**, 317–332 (2004).

14. Yuan *et al.*, Osmium-catalyzed selective oxidations of methane and ethane with hydrogen peroxide in aqueous medium. *Adv. Syn. & Catal.* **349**, 1199-1209 (2007).

15. L. C. Kao, A. C. Hutson, A. Sen, Low-temperature, palladium(II)-catalyzed, solution-phase oxidation of methane to methanol derivative. *J. Am. Chem. Soc.* **113**, 700-701 (1991).

16. C. Hammond *et al.*, Direct catalytic conversion of methane to methanol in an aqueous medium by using copper-promoted Fe-ZSM-5. *Angew. Chem. Intl. Ed.* **51**, 5129-5133 (2012).

17. M. H. Ab Rahim *et al.*, Oxidation of methane to methanol with hydrogen peroxide using supported gold–palladium alloy nanoparticles. *Angew. Chem. Intl. Ed.*. **52**, 1280-1284 (2013).

18. J. A. Lopez-Sanchez *et al.*, Au–Pd supported nanocrystals prepared by a sol immobilisation technique as catalysts for selective chemical synthesis. *Phys. Chem. Chem. Phys.* **10**, 1921-1930 (2008).

19. Materials and methods are available as supporting material on Science Online.

20. A. Thetford, G. J. Hutchings, S. H. Taylor, D. J. Willock, The decomposition of H_2O_2 over the components of Au/TiO_2 catalysts. *Proc. Roy. Soc. A*. **467**, 1885-1899 (2011).

21. L. Kesavan *et al.*, Solvent-free oxidation of primary carbon-hydrogen bonds in toluene using Au-Pd alloy nanoparticles. *Science* **331**, 195-199 (2011).

22. J. Pritchard *et al.*, Effect of heat treatment on Au-Pd catalysts synthesized by sol immobilisation for the direct synthesis of hydrogen peroxide and benzyl alcohol oxidation. *Cat. Sci. Tech.* **3**, 308-317 (2013).

23. K. A. Antcliff, D. M. Murphy, E. Griffiths, E. Giamello, The interaction of H_2O_2 with exchanged titanium oxide systems (TS-1, TiO_2, [Ti]-APO-5, Ti-ZSM-5). *Phys. Chem. Chem. Phys.* **5**, 4306-4316 (2003).

24. J. Xie, J. Yu, M. Rudolph, F. Rominger, A. S. K. Hashmi, Monofluoroalkenylation of Dimethylamino Compounds through Radical–Radical Cross-Coupling. *Angew. Chem. Intl. Ed.* **55**, 9416-9421 (2016).

25. P. P. Olivera, E. M. Patrito, H. Sellers, Direct synthesis of methanol over metallic catalysts. *Surface Science* **327**, 330-357 (1995).

26. V. T. Minasyan, G. L. Grigoryan, A. B. Nalbandyan, The heterogeneous factors in the reaction of methane oxidation, initiated by hydrogen peroxide. *Oxidation Communications* **11**, 87-97 (1998).

27. V. Nizova, G. G. Suss-Fink, G. B. Shul'pin, Catalytic oxidation of methane to methyl hydroperoxide and other oxygenates under mild conditions. *Chem. Comm.* **4**, 397-398 (1997).

28. J. Oliver-Meseguer, J. R. Carbero-Antonino, I. Dominguez, A. Leyva-Perez, A. Corma, Small gold clusters formed in solution give reaction turnover numbers of 10^7 at room temperature. *Science* **338**, 1452-1455 (2012).

15

29.	J. Colby, D. I. Stirling, H. Dalton, The soluble methane mono-oxygenase of *Methylococcus capsulatus* (Bath). *Biochem. J.* **165**, 395-402 (1977).

30.	R. P. Noceti, C. E. Taylor, J. R. D'Este, Photocatalytic conversion of methane. *Catal. Today* **33**, 199-204 (1997).

31.	M. A. Gondal, A. Hameed, A. Suwaiyan, Photo-catalytic conversion of methane into methanol using visible laser. *Appl. Cat. A: General* **243**, 165-174 (2003).

32.	K. W. Frese, Jr., Partial electrochemical oxidation of methane under mild conditions. *Langmuir* **7**, 13-15 (1991).

33.	A. Tomita, J. Nakajima, T. Hibino, Direct oxidation of methane to methanol at low temperature and pressure in an electrochemical fuel cell. *Angew. Chem. Intl. Ed.* **47** 1462-1464 (2008).

Acknowlegdements

16